Structural Engineering and Mechanics, *Vol. 50, No. 4 (2014) 459-469*
DOI: http://dx.doi.org/10.12989/sem.2014.50.4.459

Failure analysis of steel column-RC base connections under lateral cyclic loading

Serhat Demir*, Metin Husem[a] and Selim Pul[b]

Department of Civil Engineering, Karadeniz Technical University, 61080, Trabzon, Turkey

(Received December 6, 2013, Revised March 2, 2014, Accepted March 5, 2014)

Abstract. One of the most important structural components of steel structures is the column-base connections which are obliged to transfer horizontal and vertical loads safely to the reinforced concrete (RC) or concrete base. The column-base connections of steel or composite steel structures can be organized both moment resistant and non-moment resistant leading to different connection styles. Some of these connection styles are ordinary bolded systems, socket systems and embedded systems. The structures are frequently exposed to cycling lateral loading effects causing fatal damages on connections like columns-to-beams or columns-to-base. In this paper, connection of steel column with RC base was investigated analytically and experimentally. In the experiments, bolded connections, socket and embedded connection systems are taken into consideration by applying cyclic lateral loads. Performance curves for each connection were obtained according to experimental and analytical studies conducted and inelastic behavior of connections was evaluated accordingly. The cyclic lateral performance of the connection style of embedding the steel column into the reinforced concrete base and strengthening of steel column in upper level of base connection was found to be higher and effective than other connection systems. Also, all relevant test results were discussed.

Keywords: embedded steel column bases; steel columns; reinforced concrete; cyclic loading; finite element analysis

1. Introduction

Traditionally in the steel structures, base systems are built concrete or reinforced concrete. For the column-base connections, columns are prepared and welded to the end plate in the factory. Then the surfaces of the columns are smoothened, and combined on the base which was prepared with bolts. In the connections, bolts and welded components are commonly used because of being used easily and saving time. However, in case of exposing to horizontal forces such as earthquakes and so on, some important damages like excessive anchor rod elongation, unexpected early anchor rod failure, shear key failure, brittle base plate fracture have been occurred (Technical Council on Lifeline Earthquake Engineering 1995, Northridge Reconnaissance Team 1996).

In column-base connections, columns directly embedded to the base or placing the columns to

*Corresponding author, Ph.D. Student, E-mail: s.demir@ktu.edu.tr
[a]Professor, E-mail: mhusem@ktu.edu.tr
[b]Associate Professor, E-mail: spul@ktu.edu.tr

http://www.techno-press.org/?journal=sem&subpage=8 ISSN: 1225-4568 (Print), 1598-6217 (Online)

the hole which were left empty during the building process and stabilizing using different bindings are the most valid methods. In these systems, the structure forms a composite system because of co-working of steel and reinforced concrete. Because of their rigidity, resistance and ductility, composite structure systems have adequate seismic performance. Besides, they also decrease the cost of especially multi-storey structures (Broderick and Elnashai 1996, Lee and Pan 2001, Ricles and Paboojian 1994).

In the classic calculations of steel members connections, connections between contact surfaces are considered as a connector which can transfer moment. Recently, this has been commonly used in steel column-base connections. However, when the moment of applied load affect in an increasing way of shear and tensile force, this approach is inadequate to explain the real behavior of contact surface between column-base connections (Kontoleon *et al.* 1999). Laboratory studies and practical applications have shown that separation has been between the deformed column end plate and contact surface of concrete base (Sarno *et al.* 2007). This attracts the attention of researchers who study based on analytic, experimental and numerical approach. Studies based on analytic approach showed that normal reaction distributions which were seen on the column-base effective contact surface, were formed because of concentric and low capacity loading (Fling 1970, Murray 1983). Intensive experimental studies which aimed certain definition and evaluation of the behavior of column-base connections are occurred under the concentric and eccentric loading (Dewolfe 1978, Cook and Klinger 1992). Up to now, lots of experimental (Akiyama *et al.* Kallolil *et al.* 1998, Morino *et al.* 2003, Nagasima and Igarashi 1986, Pertold *et al.* 2000) and numerical (Stamatopoulos and Ermopoulos 2011, Nakashima 1992, Ermopoulos and Stamatopoulos 1996) studies on embedment length, base plate size and shape, depth and number of anchor rods, end detail were done.

In this study, the connections between steel column and reinforced concrete base were examined experimentally and analytically. In the experiments, connections were done embedding and using anchor bolts and sockets. Loading was applied horizontal and cyclic on steel columns. At the end of experimental and analytical studies, different performance curves were obtained from each test member. Based on these curves, inelastic behaviors of each connection were evaluated. As a result, connection behavior of embedded system was defined more proper comparing to other systems.

2. Experimental program

2.1 Specimens and test setup

In this study, 12 test specimen (3 for each connection) was produced to investigate the effect of different types of steel column-base connections on horizontal load carrying capacity and inelastic behavior of columns. Test specimens have 700×700 mm base sections with 400 mm high. RC base system and its reinforcement details are given in Fig. 1.

In the production of reinforced concrete bases, aggregate, maximum size 16 mm, and CEM II/A-P 32.5 N type cement was used. Water/cement ratio (*w/c*) and amount of cement is 0.45 and 350 kg/cm^3 in the produced concrete, respectively. For each base, three standard cylinder specimens of produced concrete was taken, and for 28 days, they were covered to be kept wet like RC bases. Experiments were done in 28 days. Uniaxial compressive test were done on the standard cylinder specimens and 34.8 MPa pressure strength was obtained. Steel columns which were

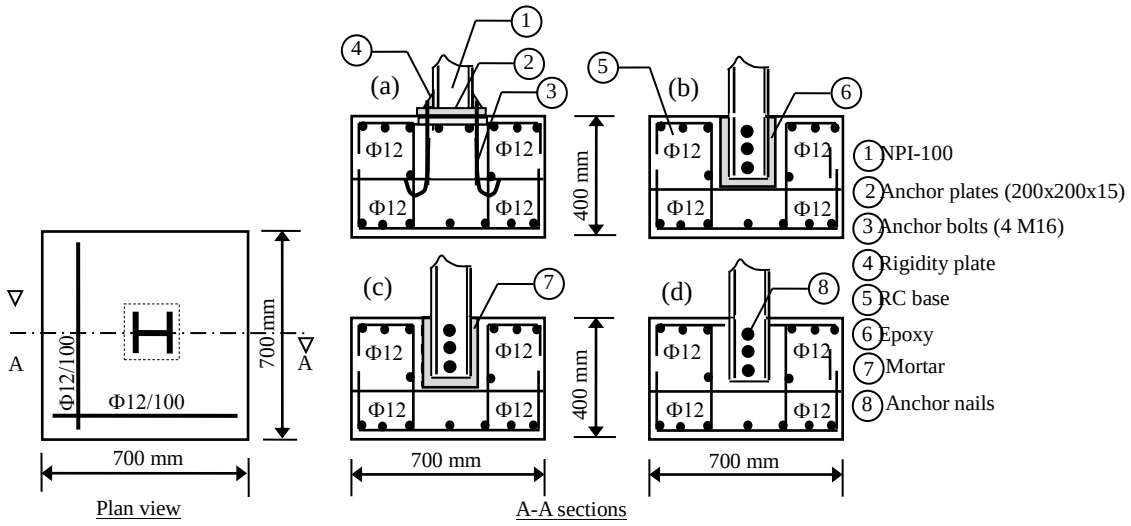

Fig. 1 Plan and cross-sectional view of RC base

Table 1 Results of tensile coupon test

Location	Thickness (mm)		Yield stress (MPa)	Ultimate stress (MPa)	Elongation at rupture (%)
	Nominal	Actual			
Column flange	6.8	6.83	248.8	425.1	25.7
Column web	5.5	5.57	255.3	441.6	24.8
M16 anchor	-	-	324.6	478.3	23.5
Bolt	-	-	774.6	1048.3	28.5
Plates	15	15.13	277.4	449.9	24.1
ø12 rebar	-	-	487.2	564.6	23.3

connected to RC base in four different types was chosen from I-shape profiles with 100 mm cross-section height (I100). The average results of the coupon tests for the steel members used in this test are presented in Table 1. Three coupons were tested for each material.

For the 1st series of experiments (E1) as shown in Fig. 1(a); four anchors with 16 mm diameter (M16) were put into the base system with 200 mm part insert the base. To prevent pull away of these anchors, a hook was put in one end. Then, the prepared concrete was poured in to the base mold in three phases. After the concrete waited for 28 days (after it gained strength) a steel base plate with 15 mm thickness and 200x200 mm cross section was put on RC base. Steel columns with 400 mm length were welded on steel end plate with 15 mm thickness and 200×200 mm cross section. Than steel column RC base connections done with bolts (Figs. 1(a) and 2). The connection between the steel column and end plate was strengthened using rigidity plate (triangle steel plates) in the four sides of column.

For the second series of experiments (E2), while building the RC base a socket hole was left to make the column 200 mm embedded (Fig. 1(b)). The RC base which was prepared in that way was kept waiting for 28 days to gain strength. Later, in order to increase adherence, 500 mm anchor nails were welded straight to the axis of column, on the column's part which was inside the socket. After prepared column was set into the RC base, the connection was completed using montage

Fig. 2 Test specimens and set-up

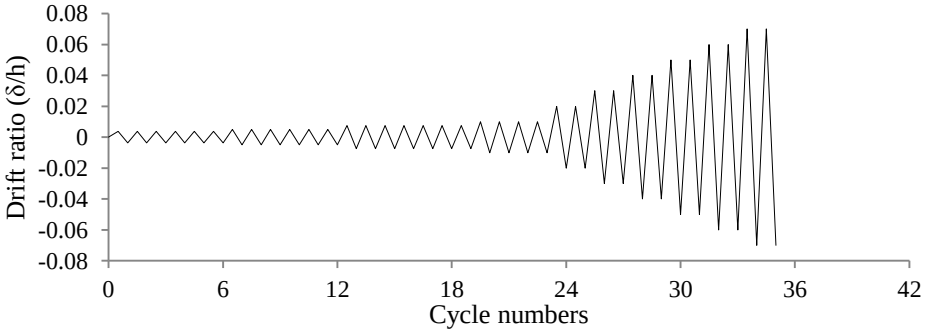

Fig. 3 Loading protocol in accordance with FEMA350 (2000)

mortar which had three component Masterflow 402 solvent free, epoxy resin, formed by hardening and special granulations quartz aggregates, having really high resistance to static and dynamic heavy loads, fitting itself (Figs. 1(b) and 2).

For the third series of experiments (E3), connection was also done as in E2 series, but 500 dose cement mortar was used instead of Masterflow (Figs. 1(c) and 2).

For the fourth series of experiments (E4), the steel column was produced together with the RC base embedded into the base (Figs. 1(d) and 2).

Test members which were ready for the experiments were stabilized to the rigid plate using four 50 mm diameter anchor members produced by high resistance steel. Later, steel columns were exposed to horizontal cyclic load (Fig. 2). The loading system consisted of a 500 kN capacity hydrolic jack and a loadcell placed in the end of it. The displacement occurred load from the end of the column was measured with the help of LVDT. Cyclic loadings were done according to the

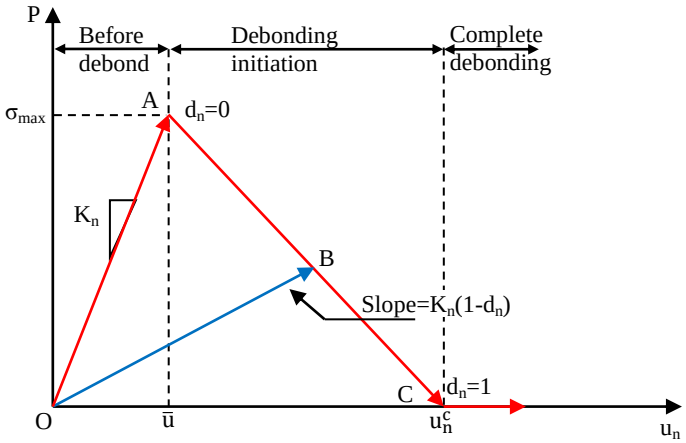

Fig. 4 Normal contact stress and contact gap curve for bilinear CZM (ANSYS 2008)

displacement controlled loading protocol which was suggested in FEMA 350 (2000) and given in Fig. 3.

3. Analytical modeling

Finite element analysis of test specimens was performed using ANSYS (2008). Material properties were defined by element type, material model and key options. Eight node solid brick elements, SOLID185, were used for three dimensional modeling which has stress stiffening, large deflection and large strain capabilities, also, having three degrees of freedom at each node: transition in the nodal *x*, *y* and *z* directions. Material models are the linear and nonlinear properties that define the elements behavior. Stress-strain relationship, modulus of elasticity, *E*, and poisson ratio, *v*, for all elements defined according to experimental results. To model the metal plasticity behavior under cyclic loading, multilinear kinematic hardening model, MKIN, were used which included Bauschinger effect. Contact surface between column and RC base were simulated with CONTA174 and TARGE170 contact pair. Connection between the contact surface of embedded steel column and RC base for E2, E3 and E4 were modeled with combining the cohesive zone material (CZM) which is proposed by Alfano and Crisfield (2001) with bonded contact option. In this study, when the tensile stress of bonding material between two surfaces is overcome, debonding is occurred. The graph which shows the opening occurring between two surfaces with normal contact stress was given in Fig. 4.

This graph can be obtained in this way

$$P=K_n u_n (1-d_n) \tag{1}$$

$$d_n = 0 \quad \text{for} \quad \Delta_n \le 1 \tag{2}$$

$$0 < d_n = \left(\frac{u_n - \bar{u}_n}{u_n} \right) \left(\frac{u_n^c}{u_n^c - \bar{u}_n} \right) < 1 \quad \text{for} \quad \Delta_n > 1 \tag{3}$$

with

$$\Delta_n = \frac{u_n}{\bar{u}_n} \tag{4}$$

Where $P, K_n, u_n, \bar{u}_n, u_n^c, d_n$ are normal contact stress (tension), normal contact stiffness, contact gap, contact gap at the maximum normal contact stress, contact gap at the completion of debonding, and debonding parameter respectively. In this graph, between *OA* points was linear elastic loading zone and when it was reached to the maximum normal tension stress (σ_{max}), debonding started between the related surfaces. The behavior of linear softening was seen between *AC*. In this zone, normal contact tensile stress decreases gradually and when it comes to *C* its value becomes zero and the opening between the surfaces are completed. In the following cyclic, on the occurring opening, no tensile stress occurred but only standard contact behavior continued. The slope of the curve between *OA*, K_n, reflected that debonding would be brittle or ductile. In the analysis, these mentioned values (σ_{max}=2.8 MPa) were defined up to the mechanical properties of concrete based on experimental observations. The appearances of the prepared analytical models were given in Fig. 5.

A static analysis was performed for each of the models and full Newton-Raphson method was used for the nonlinear analysis. For displacement controlled cyclic loading totally 44 load steps were defined. All loads steps divided into multiple substeps until the total load was achieved. As a result load deflection curves were plotted for comparison with the experimental results.

4. Result and discussion

4.1 Load-displacement relationship

Load-drift ratio curves obtained from experimental and analytical studies were given in Fig. 6. As seen in these curves, maximum load obtained from experiments; displacement values corresponding to that load; displacement values corresponding to 80% of that load were given in Table 2. In the curves given in Fig. 6, the first cyclic corresponding to each drift ratio were drawn.

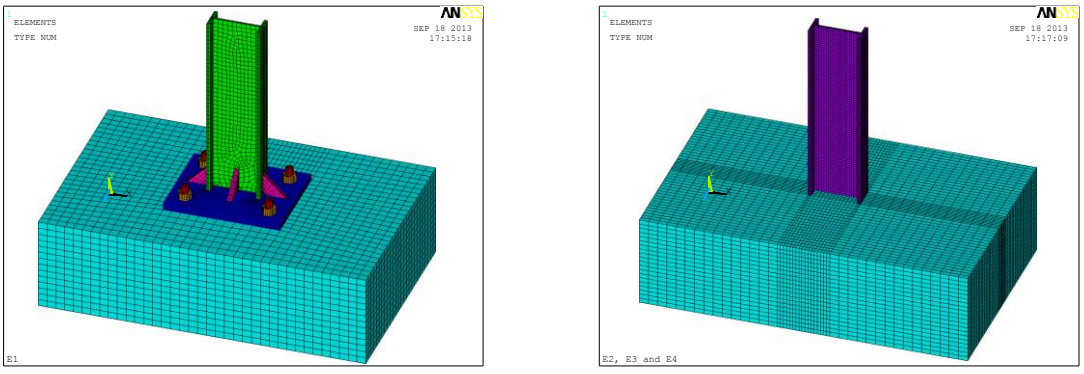

(a) (b)

Fig. 5 The developed finite element models of test specimens, (a) E1 and (b) E2, E3 and E4

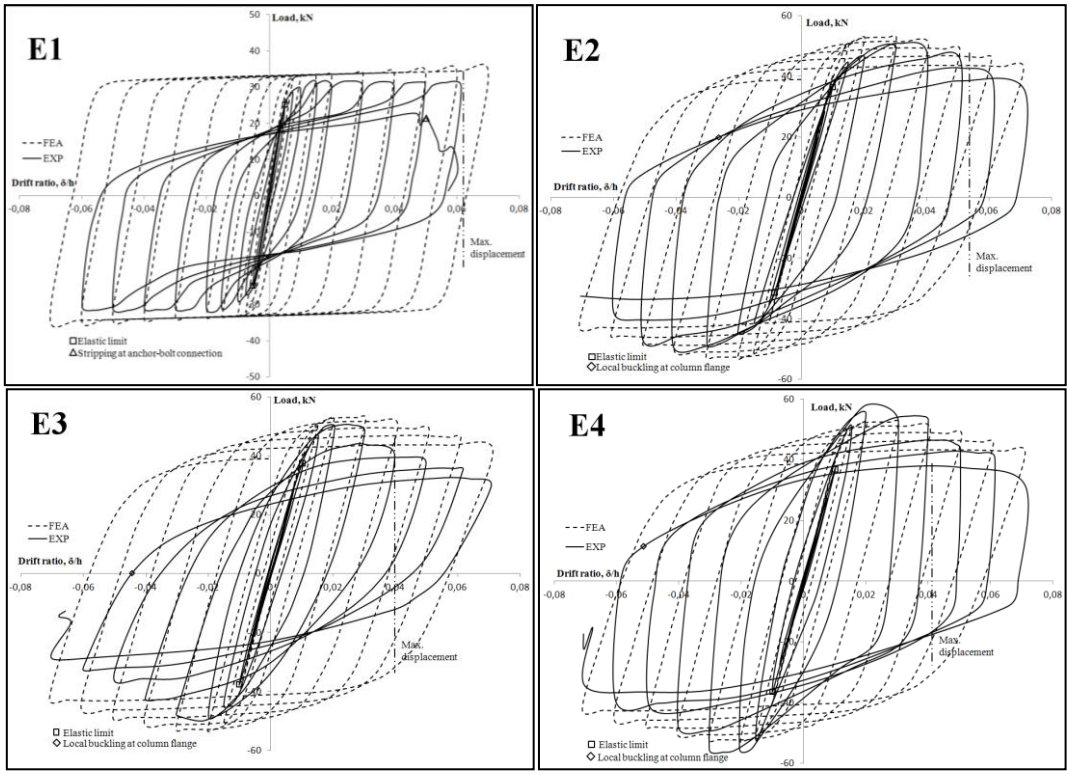

Fig. 6 Load-drift ratio relationship of test specimens

Table 2 Test results

	Maximum load						Maximum displacement					
	Positive loading (+)			Negative loading (-)			Positive loading (+)			Negative loading (-)		
Specimen	P_{max} (kN)	δ (mm)	Drift ratio[a] (%)	P_{min} (kN)	δ (mm)	Drift ratio[a] (%)	P (kN)	δ (mm)	Drift ratio[a] (%)	P (kN)	δ (mm)	Drift ratio[a] (%)
E1	31.70	7.34	1.84	31.77	6.72	1.68	30.21	24.60	6.15	30.58	23.94	5.98
E2	50.69	11.29	2.82	49.32	12.54	3.14	40.55	20.01	5.00	46.34	20.31	5.08
E3	50.47	8.91	2.32	49.93	9.42	2.35	40.38	18.83	4.71	42.40	16.06	4.02
E4	57.31	10.80	2.70	56.35	10.35	2.59	45.85	19.60	4.90	44.21	18.89	4.72

Drift ratio[a]: Ratio of displacement at maximum load to column high, (δ/h).

In the study, E4 which was embedded 200 mm in to the steel column welded straight was accepted as reference member. The RC base was produced when that steel column was inside the base. Therefore, maximum horizontal load obtained from experimental and analytical studies were 57.31 and 52.42 kN, and displacement corresponding to that loads were 10.80 and 9.87 mm (drift ratios 2.70% and 2.47), respectively. For this test member displacement corresponding to 80% of maximum load was 19.60 mm (drift ratio 4.90%).

For E1 specimen, maximum horizontal load obtained from experiment was 31.70 kN at 7.34 mm displacement and its 57% smaller than the load of reference member and its drift ratio is 33 %

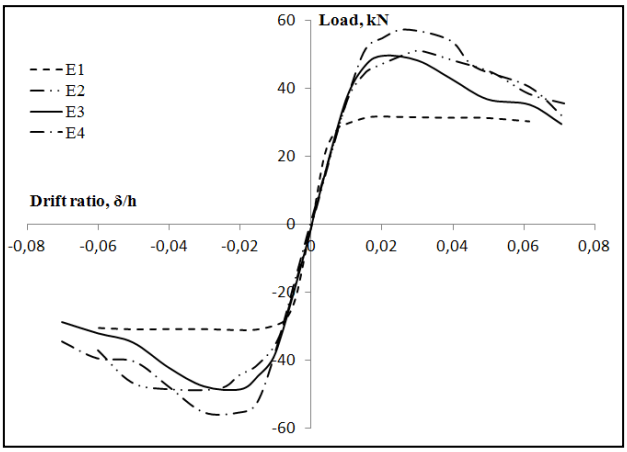

Fig. 7 Envelope curves of test specimens

smaller, respectively. The reason why this happened was column end plate and bolts reached ultimate bearing capacity before steel column. So big increases happened in the drift ratio before reaching 80% of maximum load (Fig. 6). Also maximum horizontal load obtained from analytical study was 33.64 kN with 9.18% differences according to experimental result.

For E2 and E3 specimens maximum horizontal loads obtained from experiments were 50.69 and 50.47 kN at 11.29 and 8.91 mm displacements, respectively. Between the test members prepared by using soil mixture with epoxy based mineral and soil mixture with high dose cement (E2 and E3) a big difference wasn't observed considering horizontal load bearing capacity and displacement ratio corresponding to that load. But, horizontal load bearing capacity of the test member prepared by using soil mixture with epoxy based mineral and its drift ratio was closer to the values obtained from reference member (E4). This is because soil mixture with high dose cement between steel column-base was crushed earlier than soil mixture with epoxy based mineral.

In the analytical study, maximum horizontal loads obtained for E2 and E3 were 50.69 and 50.67 kN at 11.29 and 8.91 mm displacements, respectively.

Although, there was a harmony between experimental and analytic results given in Fig. 6, there was a difference between regression curves of cyclic. Experimental and analytic results were very close to each other in the member (E4) in which steel column was produced together. The reason for this, in all three members, mechanical properties of concrete prevailed the cracks on the column-base interface, therefore, for all three members, analytic model of CZM was modeled based on the mechanical properties of concrete. CZM had no effect on maximum loading. But the studies showed that CZM curves seriously changed the initial rigidity. That's why, experimental observations were important in the CZM modeling. Envelope curves obtained from combining peak points of horizontal load-drift ratio curves were given in Fig. 7.

As seen in Fig. 7, all samples except E1 had the same behavior until 40 kN loading level. But after this level, test members had different behaviors up to column-base connection system. In the test member of E1, initial rigidity increased (13.53 kN/mm) because of the rigidity plates used to connect column to the end plate, and then, bearing capacity was lost because of bending of the end plate in a lower (app. 30 kN) loading level.

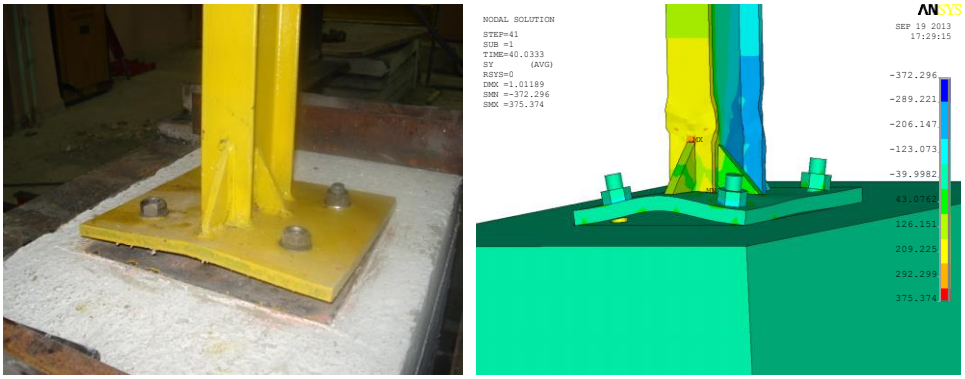

Fig. 8 Bending of end plate and stress state

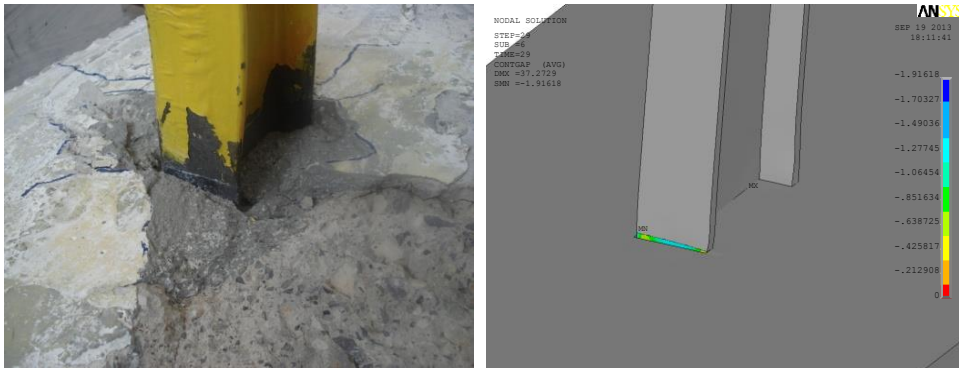

Fig. 9 Debonding, took place at the interface of steel column-RC base

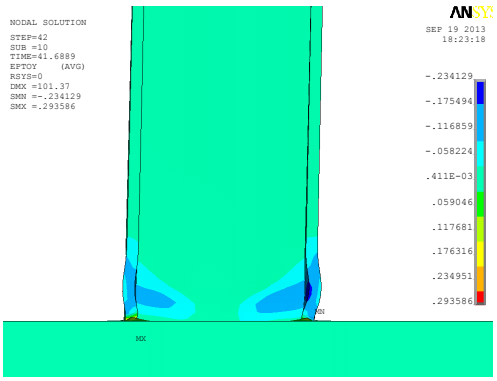

Fig. 10 In the end of experiment, local buckling took place at the column flange

4.2 Failure mechanism

Deformation status in the end plate as a result of experimental and analytic studies on the E1 series test members were given in Fig. 8. As seen in these figures, strains caused by loading were centered on the bolts. In the 26th cyclic, in approximately 11.96 mm displacement, the bending took place in the end plates. In the 29th cyclic (in approximately 20.12 mm displacement) after the

steel column reached to the yield strength, stripping took place in the bolts and therefore they lost ultimate bearing capacity.

E2 test member, prepared by placing into the base block using epoxy based binder reached at the yield strength at the upper level of steel column base earlier than E3 and E4. Before E2 experiment member reached at the maximum strength, micro cracks happened in steel column-base connection (Fig. 9). In the experiments of E2, E3 and E4 when the maximum loading level was reached, displacements increased and advanced level of deformation happened at the steel columns, and also sectional yielding took place. After this happened, because of repeated cyclic local buckling took place in the flange of the columns' cross-sections and then, column started to turn on this cross section and lost its bearing capacity (Fig. 10).

5. Conclusions

Some of the results obtained from the studies which were done to investigate steel column and RC base connections were given below.

• In all experiment series exact adherence was provided until the elastic limit of steel columns-base connections. But when loading continued in the plastic level, bolts became insufficient and buckling took place on the end plate in E1 which were prepared using anchor bolts and steel end plates. In the plastic phase, when the connections were needed to carry load, choosing anchor and end plate in these connections were quite important.

• In the RC base, other connections prepared using leaving socket had similar behaviors with the test member (E4) produced as monolithic. This showed that incase column-base connection is in adequate embedding depth, column-base connections behavior was as safe as the one of monolithic test member; no matter how anchor was prepared (using either epoxy based chemical connector or high dose cement soil mixture). But E4 test member prepared as monolithic with steel column and base, in the elastic and plastic phase, under repeated cyclic loads had better behavior than the other test members.

• In the moment resisting column-base connections; removing the hinge of the upper level of base was necessary to repair the damages which can take place under repeated cyclic loading like earthquake. For this, using rigidity plates in column-base connections were enough.

References

Akiyama, H., Kurosawa, M., Wakuni, N. and Nishinura, I. (1984), "Strength and deformation of exposed type of steel column bases", *J. Struct. Constr. Eng., Tran. AIJ*, **342**, 46-54.

Alfano, G. and Crisfield, M.A. (2001), "Finite element interface models for the delamination anaylsis of laminated composites", *Mech. Comput. Issue., Int. J. Numer. Meth. Eng.*, **50**, 1701-36.

ANSYS (2008), *Finite element analysis system*, SAS IP, Inc., USA.

Broderick, B.M. and Elnashai, A.S. (1996), "Seismic response of composite frames-I. Response criteria and input motion", *Eng. Struct.*, **18**(9), 696-706.

Cook, R.A. and Klinger, R.E. (1992), "Ductile multiple-anchor steel-to-concrete connections", *J. Struct. Div., ASCE*, **118**, 1645-65.

Dewolfe, J.T. (1978), "Axially loaded column base plates", *J. Struct. Div., ASCE*, **104**, 781-94.

Ermopoulos, J.C. and Stamatopoulos, G.N. (1996), "Analytical modelling of column-base plates under cyclic loading", *J. Constr. Steel. Res.*, **40**(3), 225-38.

FEMA (2000), *Recommended seismic design criteria for new steel moment frame buildings*, Report no. FEMA-350, Federal Emergency Management Agency: California Universities for Research in Earthquake Engineering.

Fling, R.S. (1970), "Design of steel bearing plates", *Eng. J., AISC*, **7**(2), 37-40.

Kallolil, J.J., Chakrabarti, S.K. and Mishra, R.C. (1998), "Experimental investigation of embedded steel plates in reinforced concrete structures", *Eng. Struct.*, **20**(1-2), 105-12.

Kontoleon, M.J., Mistakidis, E.S., Baniotopoulos, C.C. and Panagiotopoulos, P.D. (1999), "Parametric analysis of the structural response of steel base plate connections", *Comput. Struct.*, **71**, 87-103.

Lee, T.K.L. and Pan, A.D.E. (2011), "Analysis of composite beam-columns under lateral cyclic loading", *J. Struct. Eng., ASCE*, **127**(2), 186-93.

Morino, S., Kawaguchi, J., Tsuji, A. and Kadoya, H. (2003), "Strength and stiffness of CFT semi-embedded type column base", *Proceedings of ASSCCA Conference*, Sydney, Australia.

Murray, T.M. (1983), "Design of lightly loaded steel column base plates", *Eng. J., AISC*, **20**, 143-152.

Nakashima, S. and Igarashi, S. (1986), "Behavior of steel square tubular column bases embedded in concrete footings under bending moment and shearing force, Part 1: test program and load-displacement relations", *J. Constr. Steel. Res., Tran. AIJ*, **366**, 106-118.

Nakashima, S. (1992), "Experimental behavior of encased steel square tubular column base connections", *Proceedings of the first word conference on constructional steel design, word developments*, Eds. Dowling, P., Harding, J.E., Bjorhovde, R. and Martinez-Romeo, E., Elsevier Applied Science, Acapulco.

Northridge Reconnaissance Team (1996), "Earthquake spectra, Northridge earthquake of January 17, 1994", *Reconnaissance Report, Supplement C-2*, **11**, 25-47.

Pertold, J., Xiao, R.Y. and Wald, F. (2000), "Embedded steel column bases - I. experiments and numerical simulation", *J. Constr. Steel Res.*, **56**, 253-70.

Ricles, J.M. and Paboojian, S.D. (1994), "Seismic performance of steel-encased composite columns", *J. Struct. Eng., ASCE*, **120**(8), 2474-94.

Technical Council on Lifeline Earthquake Engineering (1995), "Northridge earthquake-lifeline performance and post-earthquake response, monograph No. 8", ASCE, New York.

Sarno, L. Di., Pecce, M.R. and Fabbrocino, G. (2007), "Inelastic response of composite steel and concrete base column connections", *J. Constr. Steel Res.*, **63**, 819-32.

Stamatopoulos, G.N. and Ermopoulos, J.C. (2011), "Experimental and analytical investigation of steel column bases", *J. Constr. Steel. Res.*, **67**, 1341-57.